

# Inkjet-Printed Electromagnet-Based Touchpad Using Spiral Resonators

Sungjin Choi, *Student Member, IEEE*, Seunghyun Eom, Manos M. Tentzeris, *Fellow, IEEE*,  
and Sungjoon Lim, *Member, IEEE*

**Abstract**—In this paper, an inkjet-printed electromagnet-based touchpad employing spiral resonators is proposed. The proposed touchpad is fabricated by a direct patterning method using an inkjet printer with a conductive silver nanoparticle ink. The conductive patterns are easily printed on a paper substrate and sintered for achieving good conductivity. The proposed touchpad is composed of two spiral resonators that resonate at 0.94 GHz ( $f_1$ ) and 1.83 GHz ( $f_2$ ), respectively. When the first resonator is touched,  $f_1$  decreases from 0.94 to 0.81 GHz because of electromagnetic (EM) coupling between the finger and the spiral resonator. Similarly, when the second resonator is touched,  $f_2$  decreases from 1.83 to 1.55 GHz. Owing to the EM coupling distance between the spiral resonator and the finger, the frequency changes although the finger does not reach beyond a height of 1.27 mm on the spiral resonator. The performance of the proposed touchpad is validated using simulation and measurement results. [2016-0035]

**Index Terms**—Inkjet-printed electronics, paper electronics, printed electronics, spiral resonator, touch sensor.

## I. INTRODUCTION

RECENTLY, paper-based electronics have facilitated the production of cost-effective and flexible electronic devices for disposable biosensors, touch sensors, and smart packaging [1]. Most paper-based electronics require information to be acquired from external sources for various purposes such as identifying tags and sensing touch. Therefore, the implementation of touch-based electronics on paper substrates is required [2]. Several studies have tried to achieve high-performance printable touch sensors and devices [3], [4]. Although piezoresistive, piezoelectric, and capacitive sensing methods have been widely used for realizing flexible touch sensors, fabricating them onto paper substrates using a simple and cost-effective method remains a challenge [2]. Technologies for the indirect patterning of conductive materials on general substrates such as FR4 epoxy and Rogers

RT Duroid, as well as on silicon substrates have been used for imprinting conductive patterns by micro-transfer stamping [5] or photolithography [6] combined with metal evaporation and metal liftoff processes. However, in these processes, environments including chemical etching, vacuum, high temperature, and pressure are required. Recently, the demand for flexible and cheap electronic devices has increased [7]. Accordingly, flexible substrates such as polymers and paper have received considerable attention. However, these flexible substrates cannot endure the harsh environments of the indirect patterning technologies. To overcome these restrictions of indirect patterning technologies, patterning of conductive material directly onto a flexible substrate has been thoroughly studied [8]–[15]. Technologies for direct patterning of conductive material on paper substrates have been developed for paper-based electronics. Among the various conductive materials, silver nanoparticle ink in particular has been used because it can be easily patterned by an inkjet printer and becomes conductive by a simple sintering process. Silver nanoparticles can be melted together by annealing at a considerably lower temperature than the bulk metal because the melting point of the silver nanoparticle is lower than that of the bulk metal [16]. After annealing, the melted silver nanoparticles form a continuous conductive structure and the conductivity is increases. Therefore, media such as paper and film, that can burn or melt at low temperatures, can be used as substrates for patterning the electronics to implement flexible electronic devices [17]. Of late, there have been several studies for fabricating touch sensors and touchpads using inkjet-printing, chemical etching processes [18], direct writing [19] and screen-printing [20]. However, most resistive or capacitive touchpads work at low frequencies such as kilohertz waves.

In this paper, we introduce microwave resonators for touchpad applications. Owing to the high frequencies of the gigahertz waves, the proposed touchpad can detect a finger even though it is not directly touched. In addition, the size can be miniaturized because the electrical length decreases at higher frequencies. The design process of the touchpad and the inkjet printing technologies for the direct patterning of conductive material are introduced. The proposed touchpad consists of a microstrip line and two spiral resonators for the two resonant frequencies. When one of the spirals is touched, its resonant frequency changes because electromagnetic (EM) coupling occurs between the finger and the spiral resonator. The performance of the proposed touchpad is validated using simulation and measurement results.

Manuscript received February 23, 2016; revised July 15, 2016; accepted July 20, 2016. Date of publication August 3, 2016; date of current version September 29, 2016. This work was supported in part by the National Research Foundation of Korea through the Korean Government (MSIP) under Grant 2014R1A2A1A11050010, and in part by the 2015 Chung-Ang University Research Grants. Subject Editor G. Stemme.

S. Choi, S. Eom, and S. Lim are with the School of Electrical and Electronics Engineering, College of Engineering, Chung-Ang University, Seoul 06974, South Korea (e-mail: 0625csj@naver.com; umsh0303@gmail.com; sungjoon@cau.ac.kr).

M. M. Tentzeris is with the School of Electrical and Computer Engineering, Georgia Institute of Technology, Atlanta, GA 30332 USA (e-mail: emmanouil.tentzeris@ece.gatech.edu).

Color versions of one or more of the figures in this paper are available online at <http://ieeexplore.ieee.org>.

Digital Object Identifier 10.1109/JMEMS.2016.2593956

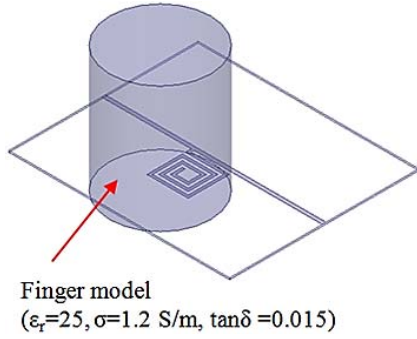


Fig. 1. Schematic view of a spiral resonator and finger model with the EM parameters for a full-wave analysis.

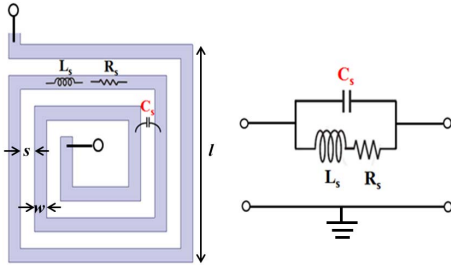


Fig. 2. Layout and equivalent circuit model of a spiral resonator.

## II. TOUCHPAD DESIGN

The proposed touchpad is composed of a microstrip line and two spirals that resonate at different frequencies and are directly connected to the microstrip line. When a user touches a spiral, its resonant frequency changes as a result of EM coupling with the finger. Fig. 1 illustrates a single spiral resonator and a finger model. A finite-element-method (FEM)-based ANSYS high frequency structure simulator (HFSS) is used for the EM simulation. The microstrip line and spiral resonators are designed on a photo-paper substrate with a thickness of 0.254 mm. The relative permittivity and loss tangent of the paper substrate are obtained as 3.1 and 0.06, respectively. The dielectric constant and loss tangent of the finger model are 25 and 0.015, respectively [21]. In addition, a finger model with a conductivity of 1.2 S/m is used for the EM simulation. The radius and height of the finger model are 8 mm and 20 mm, respectively.

The equivalent circuit model of the spiral resonator is illustrated in Fig. 2. The length of the spiral metal lines determines  $L_s$  and the gap between the spiral metal lines determines  $C_s$ . Because the resonant frequency is determined by

$$f = \frac{1}{2\pi \sqrt{L_s C_s}}, \quad (1)$$

the spiral resonator can be designed using the analytic equations for  $L_s$  and  $C_s$ . The spiral inductance and parasitic capacitance can be calculated from [22] and [23] as

$$L_s = \frac{\mu_0}{2\pi} I_{avg}^{SR} \left[ \ln\left(\frac{l_{avg}^{SR}}{2w}\right) + \frac{1}{2} \right] \quad (2)$$

$$C_s = \frac{l}{4(w+s)} \frac{N^2}{N^2+1} \times \left[ l(N-1) - \frac{N^2-1}{2}(w+s) \right] C_0 \quad (3)$$

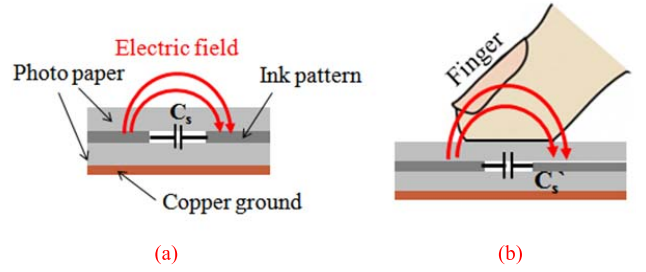


Fig. 3. (a) Cross-sectional view of the proposed touchpad. The top of the photo paper is inkjet-printed and the bottom of the photo paper is covered by copper. (b) Illustration of the touchpad with a finger.

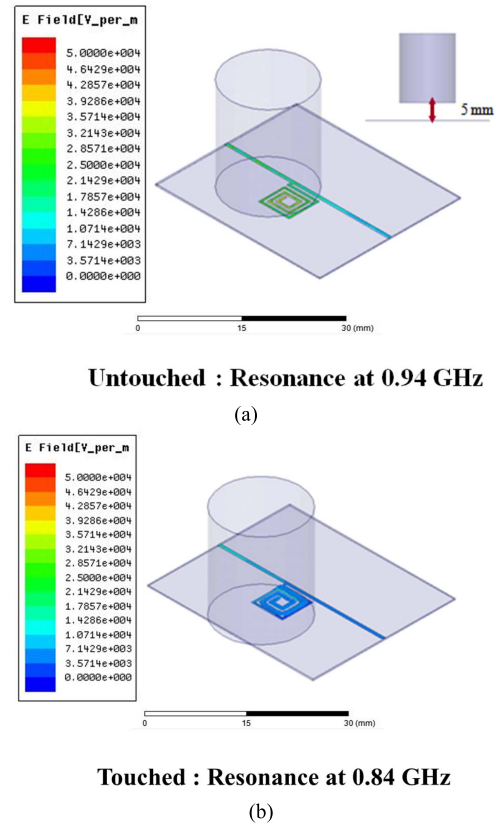


Fig. 4. Simulated electric field distribution of the spiral and finger model when (a) the finger does not touch (the finger modeled is placed 5mm above the paper) and (b) the finger touches.

where  $l$  is the side length of the external turn,  $N$  is the number of turns of the spiral resonator,  $s$  is the separation between two adjacent turns,  $C_0$  is defined for a multiple spiral resonator, and  $I_{avg}^{SR} = 4l - [2(N+1) - 3/N](s+w)$  is the average length of the spiral turn. In this work, two spiral resonators are designed to resonate at 0.94 GHz and 1.83 GHz, respectively.

When a finger touches the spiral, the electric field lines pass through the finger as shown in fig. 3. Therefore, both the effective permittivity and the capacitance change. Simultaneously, the resonant frequency of the spiral resonator also changes.

The simulated electric field distribution is shown in fig. 4. When the spiral is untouched, it resonates at 0.94 GHz ( $f_1$ ). However, when the spiral is touched, it resonates at 0.84 GHz

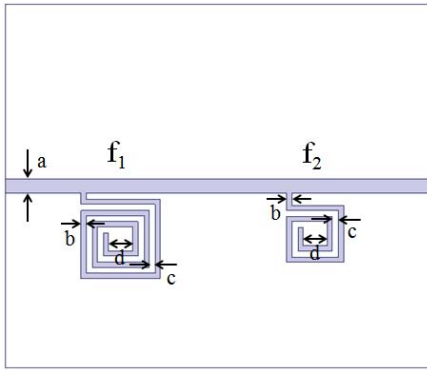


Fig. 5. Proposed touchpad with two spiral resonators for different resonant frequencies ( $a = 1.2$ ,  $b = c = 0.5$ ,  $d = 2$ ) [units: mm].

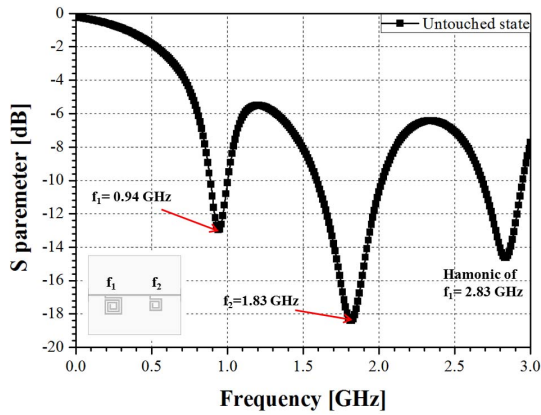


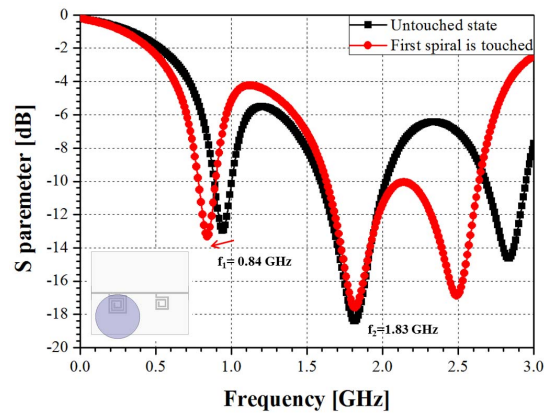
Fig. 6.  $S_{21}$  simulation result with two spiral resonators, when the proposed touchpad is untouched.

because EM coupling occurs between the spiral and the finger model. For two-touch areas, another spiral resonator is added. It resonates at 1.83 GHz ( $f_2$ ). Fig. 5 shows the proposed touchpad with two spiral resonators for different resonant frequencies. When a spiral is touched, the frequency variation is large because of the strong EM coupling. To prevent strong EM coupling between the spiral and the finger model as well as the duplication of the resonant frequencies between  $f_1$  and  $f_2$ , an additional layer of paper is placed on the designed touch sensor. The paper on the touch sensor reduces its sensitivity. However, a sufficient change in the frequency is achieved.

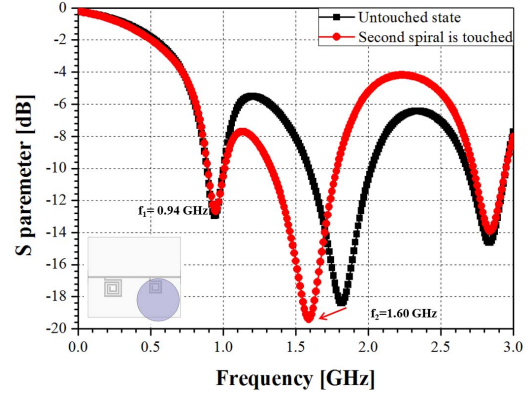
### III. SIMULATION RESULTS

Fig. 6 shows the simulation results of the insertion loss ( $S_{21}$ ) with two spiral resonators, when the proposed touchpad is untouched. The first spiral resonates at 0.94 GHz ( $f_1$ ) and the second at 1.83 GHz ( $f_2$ ). Because of the third harmonic of  $f_1$ , an additional pole exists at 2.83 GHz. To avoid the duplication of the resonant frequency when a spiral is touched, the second spiral is designed to have a resonant frequency of 1.83 GHz. This frequency is almost in the center of 0.94 - 2.83 GHz.

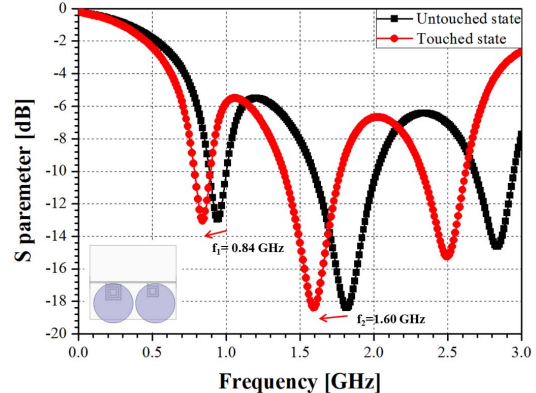
Fig. 7(a) shows the simulation results of  $S_{21}$ , with the first spiral resonator touched and the second untouched. When the first spiral is touched, the resonant frequency,  $f_1$ , decreases from 0.94 to 0.84 GHz, and the second resonant frequency,  $f_2$ ,



(a)



(b)



(c)

Fig. 7.  $S_{21}$  simulation results with (a) a touched first spiral resonator and an untouched second spiral resonator, (b) an untouched first spiral resonator and a touched second spiral resonator and (c) touched first and second spiral resonators.

does not change. Although the third harmonic of  $f_1$  also changes, it does not affect the second resonant frequency,  $f_2$ . Fig. 7(b) shows the simulation results of  $S_{21}$  with an untouched first spiral resonator and a touched second spiral resonator. When the second spiral is touched, the resonant frequency,  $f_2$ , decreases from 1.83 to 1.60 GHz. In addition, the first resonant frequency,  $f_1$ , and third harmonic of  $f_1$  do not change. Fig. 7(c) shows the simulation results of  $S_{21}$  when the first and second spiral resonators are simultaneously touched. Both  $f_1$  and  $f_2$  decrease from 0.94 GHz to 0.84 GHz and from 1.83 GHz to 1.60 GHz, respectively. To identify the effects of the sensitivity when a paper is loaded on the proposed

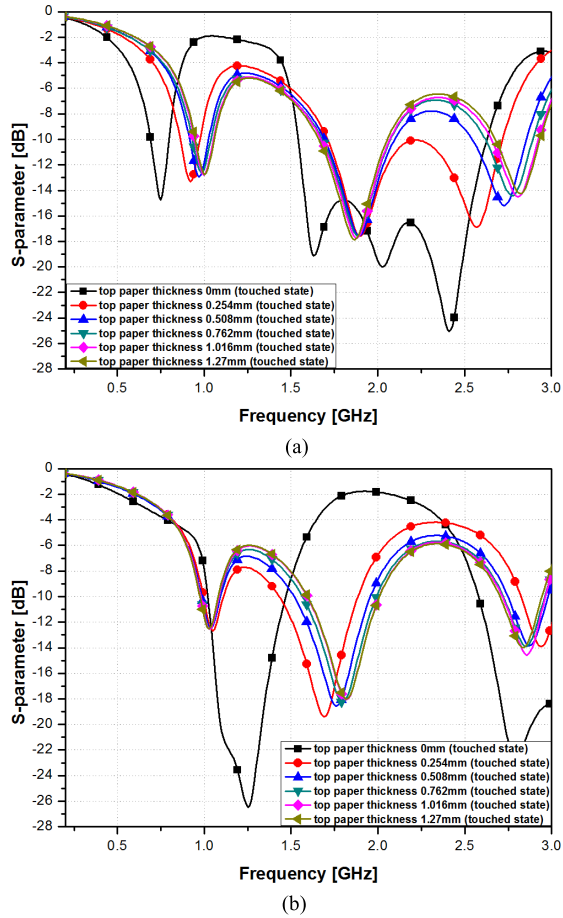


Fig. 8.  $S_{21}$  simulation results using various quantities of sheets of the top paper, when (a) the first spiral resonator is touched and (b) the second spiral resonator is touched.

touchpad, the S-parameters of the paper are simulated using various quantities of sheets of the top paper on the touchpad.

Fig. 8(a) shows the plotted simulation results of  $S_{21}$  when only the first spiral resonator is touched. Fig. 8(b) shows the plotted simulation results of  $S_{21}$  when only the second spiral resonator is touched. It is obvious that the relative frequency change ( $\Delta f/f_{\text{untouched}}$ ) decreases with a thicker top paper; for instance,  $f_1$  decreases from 0.96 to 0.63 GHz when the first button of the proposed paper without the top paper is touched. However,  $f_1$  decreases from 0.94 to 0.84 GHz when the first button of the proposed paper is touched, with a single sheet of top paper (0.254 mm thickness). A larger frequency change is not preferred in the proposed touchpad because the  $f_{2,\text{touch}}$  must be between the  $f_{1,\text{untouched}}$  and  $f_{2,\text{untouched}}$ ; when the  $f_{2,\text{touch}}$  is similar to the  $f_{1,\text{untouched}}$ , detecting the button that is touched is difficult.

#### IV. FABRICATION PROCESS

We have designed the touchpad using inkjet printing technology. First, a 1.3- $\mu\text{m}$ -thick conductive pattern is printed on a sheet of 0.254-mm-thick Kodak photo paper (Office Depot, USA), utilizing an ANP Silver Jet 55 LT-25C silver nanoparticle ink (Advanced Nano Products, Sejong, Korea) and a Dimatix DMP-2831 printer (Fujifilm Dimatix, Santa Clara, CA, USA) with a 10-pL cartridge and a drop spacing

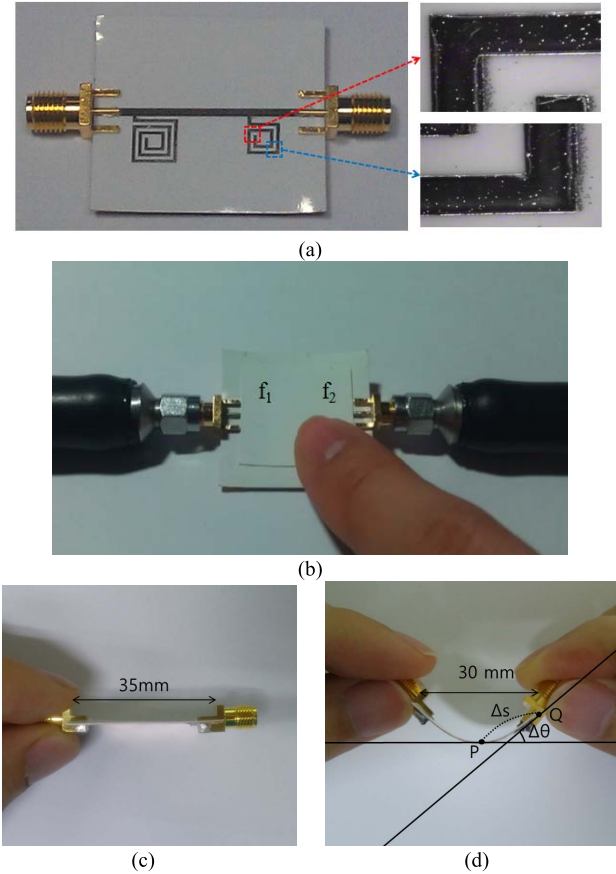


Fig. 9. (a) Fabricated prototype of the proposed touchpad, (b) touchpad when a spiral is touched, (c) side view of the flat touchpad, and (d) side view of the bent touchpad at  $k = 0.0192$ .

of 20  $\mu\text{m}$ . For high conductivity, three layers of silver nanoparticle ink are printed [23]. The touchpad is then cured for 2 h at 120  $^{\circ}\text{C}$ . Fig. 9 shows the fabricated prototype of the proposed touchpad. It also shows a photograph of the paper when a spiral is touched. SMA connectors for measurement purposes are attached using silver epoxy.

#### V. MEASUREMENT RESULTS

To demonstrate the performance of the fabricated touchpad, the S-parameters are measured using an Anritsu MS2038C network analyzer. Fig. 10(a) shows the measurement results of  $S_{21}$  with two untouched spiral resonators. The first spiral resonates at 0.94 GHz ( $f_1$ ) and the second at 1.83 GHz ( $f_2$ ). The third harmonic of  $f_1$  appears at 3.12 GHz. These results are similar to the simulation results. Fig. 10(b) shows the  $S_{21}$  measurement results when the first and second spiral resonators are simultaneously touched. When the two spirals are touched, the resonant frequency  $f_1$  decreases from 0.94 to 0.81 GHz, and the resonant frequency  $f_2$  decreases from 1.83 to 1.55 GHz. Although the third harmonic of  $f_1$  decreases slightly, it does not affect the second resonant frequency.

Fig. 11(a) shows the measurement results of  $S_{21}$  with the first spiral resonator touched and the second spiral resonator untouched. When the first spiral is touched, the resonant

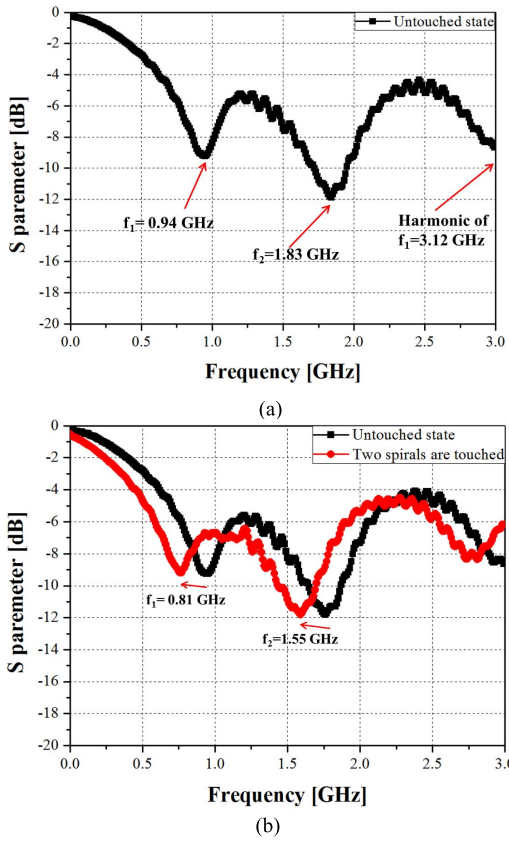


Fig. 10. Measurement results of  $S_{21}$  with both the spiral resonators (a) untouched and (b) touched.

frequency  $f_1$  decreases from 0.94 to 0.81 GHz, and second resonant frequency  $f_2$  does not change. Although the third harmonic of  $f_1$  also changes, it does not affect the second resonant frequency  $f_2$ . Fig. 11(b) shows the measurement results of  $S_{21}$  with an untouched first spiral resonator and a touched second spiral resonator. When the second spiral is touched, the resonant frequency  $f_2$  decreases from 1.83 to 1.55 GHz, and the first resonant frequency  $f_1$  does not change.

We tested the performances of the proposed touchpad when it is bent, as shown in Fig. 9(d). The curvature ratio ( $k$ ) is defined as,

$$k = \lim_{\Delta s \rightarrow 0} \left| \frac{\Delta \theta}{\Delta s} \right| = \left| \frac{d\theta}{ds} \right| \quad (4)$$

where  $\Delta s$  and  $\Delta \theta$  are the lengths of P and Q and angle of the two tangent lines, respectively. The proposed touchpad maintains its resonant frequency up to  $k = 0.0192$ . The resonant frequency changes when  $k \Rightarrow 0.0192$ .

Fig. 12(a) shows the measurement results of  $S_{21}$  with the first spiral resonator when the top paper thickness changes. When the top paper thickness is 0.254 mm,  $f_1$  decreases from 0.94 to 0.81 GHz with 14.86% sensitivity. When two sheets of top paper are loaded on the fabricated touchpad, the top paper thickness increases to 0.508 mm and  $f_1$  decreases from 0.93 to 0.83 GHz. The sensitivity for the first spiral resonator decreases with a thicker top paper. Fig. 12(b) shows the measurement results of  $S_{21}$  with the second spiral resonator,

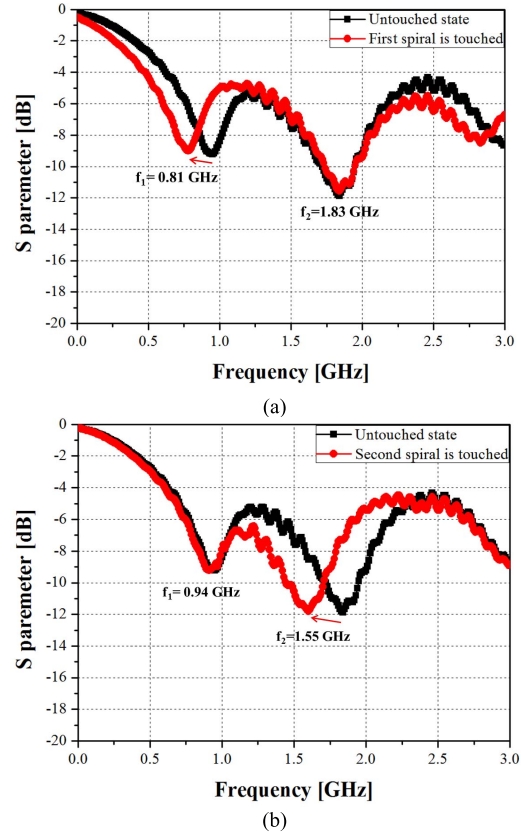


Fig. 11. Measurement results of  $S_{21}$  with (a) the first spiral resonator touched and the second spiral resonator untouched, and (b) the first spiral resonator untouched and second spiral resonator touched.

TABLE I  
MEASUREMENT RESULTS OF THE FABRICATED TOUCHPAD  
WITH DIFFERENT TOP PAPER THICKNESSES

Top paper thickness [mm]	$f_{1,touch}$ [GHz]	$f_{1,untouch}$ [GHz]	Sensitivity at $f_1$ [%]	$f_{2,touch}$ [GHz]	$f_{2,untouch}$ [GHz]	Sensitivity at $f_2$ [%]
0.254	0.81	0.94	14.86	1.55	1.83	16.57
0.508	0.83	0.93	11.36	1.65	1.78	7.58
0.762	0.84	0.92	9.09	1.68	1.76	4.65
1.016	0.84	0.92	9.09	1.68	1.76	4.65
1.270	0.84	0.92	9.09	1.68	1.76	4.65

when the top paper thickness changes. When the top paper thickness is 0.254 mm,  $f_2$  increases from 1.55 to 1.83 GHz with a 16.57% sensitivity. When the top paper thickness is 0.508 mm,  $f_2$  decreases from 1.78 to 1.65 GHz with a 7.58% sensitivity. The sensitivity of the second spiral resonator also decreases with a thicker top paper. In table I, the measurement results of the resonant frequency and the sensitivity are listed when the top paper thicknesses are 0.254, 0.508, 0.762, 1.016, and 1.270 mm, respectively. The resonant frequency remains almost unchanged when more than two sheets of top paper (0.508 mm) are used.

Owing to EM coupling between the spiral resonator and the finger, the resonant frequency shifts although the finger does not directly touch on the spiral resonator. In order to find the maximum height above the proposed touchpad, the

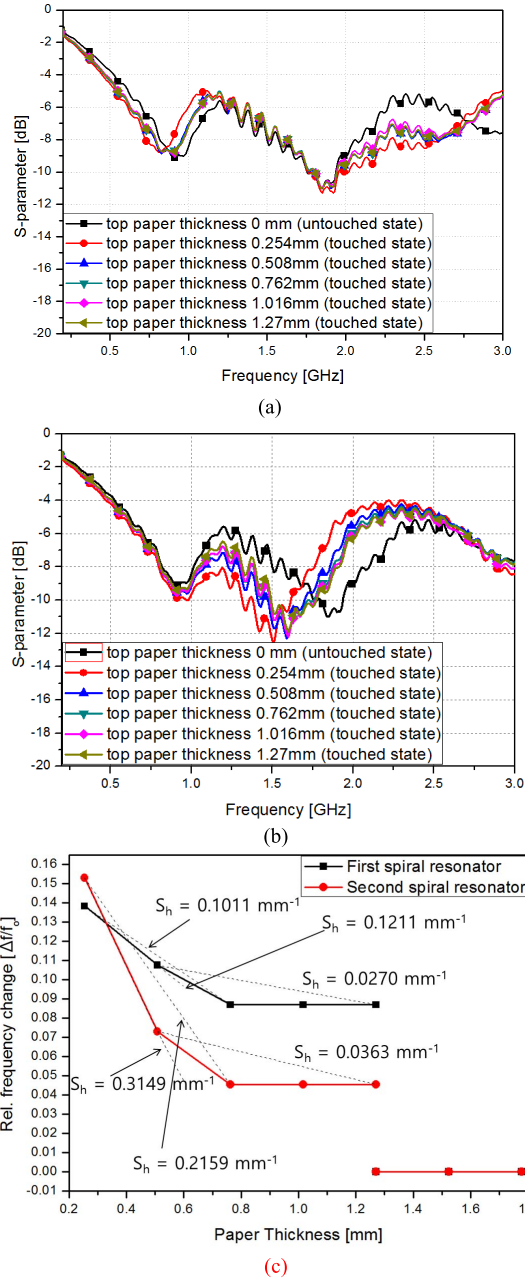


Fig. 12. Measurement results of  $S_{21}$  with changes in the top paper thickness for (a) the first spiral resonator and (b) the second spiral resonator. (c) Relative frequency change of the touchpad at different paper thicknesses.

proposed touchpad is covered by top paper with a thickness ( $h$ ) of 0.254 mm. The height is controlled by the number of top papers. For instance, two top papers on the touchpad represent a thickness of 0.508 mm above the touchpad. If the height increases, the coupling between the spiral resonator and finger becomes weaker. The resonant frequency does not change at heights greater than 1.27 mm. The relative frequency change ( $\Delta f/f_0$ ) becomes constant at heights above 0.762 mm.

In this work, the height sensitivity ( $S_h$ ) is defined as the slope of the traces in Fig. 12(c).

$$S_h = \frac{\delta(\Delta f/f_0)}{\delta h} \left[ mm^{-1} \right] \quad (5)$$

TABLE II  
COMPARISON OF OTHER PAPER-BASED TOUCHPADS

	Proposed pad	[16]	[17]	[18]
Fabrication method	Inkjet-Printing	Chemical Etching	Direct Writing	Screen-Printing
Conductive Materials	Silver nanoparticle ink	Metallized paper	Silver nanowire ink	Zinc oxide nanowire
Number of Buttons	2	10	4	10
Sensing Method	Capacitance	Capacitance	Capacitance	Resistance
Untouched State	1.83 GHz and 0.94 GHz	30–55 pF	3–4 pF	0 V
Touched State	1.55 GHz and 0.81 GHz	1000–3000 pF	20–21 pF	-3.5 V–3.5 V
Relative change	$\Delta f/f_0 = 0.153$	$\Delta C/C_0 = 46.0588$	$\Delta C/C_0 = 4.8571$	3.5 V
Height sensitivity	0.3149 mm <sup>-1</sup>	N/A	N/A	N/A

Table II shows a comparison with other paper-based touchpads. Because the proposed touchpad is based on EM resonance, it can detect touch states by the change in the resonant frequencies, while the other touchpads detect touch states by changes in the capacitance or resistance. The relative change in the proposed touchpad is smaller than those in other capacitive and resistive touchpads. However, the proposed touchpad has an advantage of non-contact detection compared to the other technologies.

## VI. CONCLUSION

In this study, we have proposed an inkjet-printed, electromagnet-based touchpad using two spiral resonators. The proposed touchpad is composed of a microstrip line with two directly connected spiral resonators. These two spirals resonate at different frequencies of 0.94 and 1.83 GHz, respectively. When a particular spiral is touched, its resonant frequency changes because EM coupling occurs between the finger and the spiral resonator. Simultaneously, the untouched spiral resonant frequency does not change. The proposed touchpad was implemented using inkjet printing technologies and its performance was validated using the simulation and measurement results. The proposed touchpad can be applied to paper-based instruments, audio books, and for disposable paper-based tag applications.

## REFERENCES

- [1] D. Tobjörk and R. Österbacka, "Paper electronics," *Adv. Mater.*, vol. 23, no. 17, pp. 1935–1961, May 2011.
- [2] J. Kim, J. H. Jong, and W. S. Kim, "Repeatedly bendable paper touch pad via direct stamping of silver nanoink with pressure-induced low-temperature annealing," *IEEE Trans. Nanotechnol.*, vol. 12, no. 6, pp. 1139–1143, Nov. 2013.
- [3] K. Kordás *et al.*, "Inkjet printing of electrically conductive patterns of carbon nanotubes," *Small*, vol. 2, nos. 8–9, pp. 1021–1025, Aug. 2006.
- [4] S. Chung *et al.*, "Flexible high-performance all-inkjet-printed inverters: Organo-compatible and stable interface engineering," *Adv. Mater.*, vol. 25, no. 34, pp. 4773–4777, 2013.
- [5] K. J. Stevenson, G. J. Hurrst, and J. T. Hupp, "High resolution assembly of patterned metal oxide thin films via microtransfer molding and electrochemical deposition techniques," *Electrochem. Solid-State Lett.*, vol. 2, no. 4, pp. 175–177, 1999.

- [6] M. W. Knight, H. Sobhani, P. Nordlander, and N. J. Halas, "Photodetection with active optical antennas," *Science*, vol. 332, no. 6030, pp. 702–704, 2011.
- [7] D. J. Gundlach, "Organic electronics: Low power, high impact," *Nature Mater.*, vol. 6, no. 3, pp. 173–174, 2007.
- [8] Y.-L. Loo, R. L. Willett, K. W. Baldwin, and J. A. Rogers, "Interfacial chemistries for nanoscale transfer printing," *J. Amer. Chem. Soc.*, vol. 124, no. 26, pp. 7654–7655, 2002.
- [9] Y.-L. Loo, D. V. Lang, J. A. Rogers, and J. W. P. Hsu, "Electrical contacts to molecular layers by nanotransfer printing," *Nano Lett.*, vol. 3, no. 7, pp. 913–917, 2003.
- [10] J. M. Dang, J. K. Hwang, and M. M. Sung, "High-resolution patterning of silver thin films with a water-mediated metal transfer printing," *J. Nanosci. Nanotechnol.*, vol. 12, no. 2, pp. 1471–1475, 2012.
- [11] S. K. Ko *et al.*, "Direct nanoimprinting of metal nanoparticles for nanoscale electronics fabrication," *Nano Lett.*, vol. 7, no. 7, pp. 1869–1877, Jun. 2007.
- [12] I. Park *et al.*, "Nanoscale patterning and electronics on flexible substrate by direct nanoimprinting of metallic nanoparticles," *Adv. Mater.*, vol. 20, no. 3, pp. 489–496, 2008.
- [13] B. Y. Ahn *et al.*, "Omnidirectional printing of flexible, stretchable, and spanning silver microelectrodes," *Science*, vol. 323, no. 5921, pp. 1590–1593, 2009.
- [14] J. K. Hwang *et al.*, "Direct nanoprinting by liquid-bridge-mediated nanotransfer moulding," *Nat. Nanotechnol.*, vol. 5, no. 10, pp. 742–748, 2010.
- [15] B. Kang, S. Ko, J. Kim, and M. Yang, "Microelectrode fabrication by laser direct curing of tiny nanoparticle self-generated from organometallic ink," *Opt. Exp.*, vol. 19, no. 3, pp. 2573–2579, 2011.
- [16] P. R. Couchman and W. A. Jesser, "Thermodynamic theory of size dependence of melting temperature in metals," *Nature*, vol. 269, no. 5628, pp. 481–483, 1977.
- [17] A. Russo, B. Y. Ahn, J. J. Adams, E. B. Duoss, J. T. Bernhard, and J. A. Lewis, "Pen-on-paper flexible electronics," *Adv. Mater.*, vol. 23, no. 30, pp. 3426–3430, 2011.
- [18] A. D. Mazzeo *et al.*, "Paper-based, capacitive touch pads," *Adv. Mater.*, vol. 24, no. 21, pp. 2850–2856, 2012.
- [19] R.-Z. Li, A. Hu, T. Zhang, and K. D. Oakes, "Direct writing on paper of foldable capacitive touch pads with silver nanowire inks," *ACS Appl. Mater. Interfaces*, vol. 6, no. 23, pp. 21721–21729, 2014.
- [20] X. Li, Y.-H. Wang, C. Zhao, and X. Liu, "Paper-based piezoelectric touch pads with hydrothermally grown zinc oxide nanowires," *ACS Appl. Mater. Interfaces*, vol. 6, no. 24, pp. 22004–22012, Dec. 2014.
- [21] D. Choi, Y. Gimm, and J. Choi, "Manufacturing of a Korean hand phantom with human electrical properties at 835 MHz and 1,800 MHz bands," *J. Korean Inst. Electromagn. Eng. Sci.*, vol. 24, no. 5, pp. 534–540, 2013.
- [22] F. Bilotti, A. Toscano, and L. Vegni, "Design of spiral and multiple split-ring resonators for the realization of miniaturized metamaterial samples," *IEEE Trans. Antennas Propag.*, vol. 55, no. 8, pp. 2258–2267, Aug. 2007.
- [23] F. Bilotti, A. Toscano, L. Vegni, K. Aydin, K. B. Alici, and E. Ozbay, "Equivalent-circuit models for the design of metamaterials based on artificial magnetic inclusions," *IEEE Trans. Microw. Theory Techn.*, vol. 55, no. 12, pp. 2865–2873, Dec. 2007.

Authors' photographs and biographies not available at the time of publication.